 doi:10.20944/preprints201803.0099.v1

Physicochemical properties of TiO_2 nanoparticle loaded APTES-functionalized MWCNTs composites and their photocatalytic activity with kinetic study

Amirah Ahmad[1], Mohd Hasmizam Razali[1,2], Mazidah Mamat[1], Karimah Kassim[3] and Khairul Anuar Mat Amin[1,2]

[1]*School of Fundamental Sciences, Universiti Malaysia Terengganu, 21030 Kuala Terengganu, Terengganu, Malaysia.*

[2]*Advanced Nanomaterials Research Group, School of Fundamental Science, Universiti Malaysia Terengganu, 21030 Terengganu, Malaysia.*

[3]*Centre for Nanomaterials Research, Universiti Teknologi MARA, 40450 Shah Alam, Selangor, Malaysia.*

Please address all correspondence to: mdhasmizam@umt.edu.my

ABSTRACT

In this study, functionalized-MWCNTs with 3-aminopropyltriethoxysilane (APTES) loaded titania nanoparticles (MWCNTs-APTES-TiO_2) were prepared to investigate their physicochemical properties and photocatalytic activity for methyl orange (MO) degradation. The TiO_2 nanoparticles, functionalized-MNCNT and composite powders were characterized by XRD, raman, and TEM. The results obtained proved that titania (TiO_2) nanoparticles was successfully loaded on APTES-MWCNTs. The best photocatalytic degradation of methyl orange solution under UV light irradiation was recorded over MWCNTs-APTES-TiO_2 (1:2), with 87% after 180 min. Kinetic analysis indicated that photocatalytic degradation of MO solution by MWCNTs-APTES-TiO_2 obeyed second-order kinetic model ($R^2 > 0.95$), supported by half-life equations and graph. The presence of carbon nanotubes accelerated the degradation of methyl orange due to inhibition of electron-hole recombination, the formation of additional hydroxyl radicals and functional groups of the latter had an inhibitory effect on the degradation of methyl orange. This study shows

 doi:10.20944/preprints201803.0099.v1

that the MWCNTs-APTES-TiO_2 nanocomposites exhibit promising photocatalytic degradation against methyl orange.

Keywords: Photocatalyst, Titanium Dioxide, Multi-walled Carbon Nanotubes, Methyl Orange, Degradation

Introduction

Textile, food beverage, paper and other industrial dyestuff generated large quantities of dye pollutants that lead to the serious water contamination problems. The effluents discharged from these industries are usually strong colored and contribute to non-aesthetic pollution that affects to human beings and aquatic life due to their carcinogenic, toxicity, and mutagenic effects (Hoffmann et al. 1995, Legrini et al. 1993). Among those organic pollutants, methyl orange is one of the pollutants that can subsequently lead to the water contaminations problems (Haque et al. 2011). Therefore, it is important to study the removal of methyl orange in order to avoid any environmental threats.

Recently, photocatalytic degradation has attracted great attention as an effective method to purify wastewater by converting photon energy to chemical energy and cause organic contaminants can be decomposed. Titanium dioxide (TiO_2) is most frequently used in the photocatalytic process due to its chemical stability, high activity, low toxicity, water insolubility under most conditions, no secondary pollution, robustness against photocorrosion and low cost (Fujishima et al., 2000). However, there are still many challenges as a great photocatalyst because it has a wide band gap energy of 3.2 eV for anatase that enables TiO_2 to absorb only UV light with a wavelength lower than 385 nm (Pelaez et al., 2012, Wu et al., 2013). A few methods have been

 doi:10.20944/preprints201803.0099.v1

attempted in order to increase the catalytic performance of the TiO_2 photocatalyst such as metal/non-metal doping, coupling with semiconductors and dye sensitization (Chen et al., 2003, Gao et al., 2009). A previous study reported that to overcome the limitation of TiO_2 and to increase the photocatalytic activity of TiO_2 by retardation of electron-hole recombination, introduce active sites of reaction, and modification of band gap (Kubacka et al. 2011, Nainani et al. 2012).

Among the possible materials proposed for modifying TiO_2, multi-walled carbon nanotubes (MWCNTs) seems suitable materials to improve the photocatalyst performance due to their unique structure and properties (Hone et al. 2002). Besides, MWCNTs-TiO_2 composites have paying attention due to the mechanical, electrical and thermal properties of MWCNTs and also favorable application of MWCNTs-TiO_2 due to their ability to adsorb hydrophobic organic pollutants that hardly adsorbed by TiO_2 nanoparticles themselves and also high capability to conduct electrons. A previous study reported that the MWCNTs functioned as support to catalyst, provide the reactivesurface area and stabilize the charge separation by trapping the electrons transferred from TiO_2, thus thwarting the charge recombination (Zhao et al. 2013). Interestingly, the band gap energy of TiO_2 was found reduced from 3.2 to 2.79 eV with the incorporation of MWCNTs (Jiang et al. 2011).

Shitole et al. (Shitole et al. 2013) investigated the degradation of MO using TiO_2-MWCNTs as photocatalyst and they found that the rate of degradation of MO dye with TiO_2-MWCNTs was 10 times higher than to TiO_2. The highest photocatalytic degradation efficiency can be ascribed by the presence of MWCNTs which act as dispersing agent, adsorbent and electron

Preprints (www.preprints.org) | NOT PEER-REVIEWED | Posted: 14 March 2018 doi:10.20944/preprints201803.0099.v1

reservoir to facilitate the separation of the electron-hole pairs at the TiO_2-MWCNTs interface, thus leading to the faster rates of photocatalytic oxidation (Xu et al. 2010). Tan et al. (Ling Tan et al. 2015) reported that the degradation of MO in the absence MWCNTs-TiO_2 catalyst after 1 h of UV irradiation is very low because it is mainly photolysis process (Gao et al. 2009). Meanwhile, MWCNTs-TiO_2 exhibits the highest photodegradation of MO due to suppressing the recombination of photogenerated electrons and holes (Djokić et al. 2014).

This study highlights the photocatalytic degradation of methyl orange from an aqueous solution onto MWCNTs-APTES-TiO_2 nanocomposites. The MWCNTs were functionalized with 3-aminopropyltriethoxysilane (APTES) to improve their solubility and dispersion capabilities prior to use (Harris 2009). In our previous study, we reported the adsorption of MO using MWCNTs-APTES-TiO_2 and found high adsorption abilities against methyl orange in 60 min (Ahmad et al. 2017). Thus, it is expected that MWCNTs-APTES-TiO_2 showed better photocatalytic performance as compared to pure TiO_2. In this study, MWCNTs were synthesized using chemical vapor deposition (CVD) method, functionalized with APTES and then were loaded with TiO_2. The synthesized materials were characterized using XRD, Raman, TEM and EDX. Next, the kinetic of zero-order, first-order and second-order were then studied to understand the specific degradation of the samples.

Experimental

Synthesis of MWCNTs-APTES-TiO_2 composites

Preprints (www.preprints.org) | NOT PEER-REVIEWED | Posted: 14 March 2018 doi:10.20944/preprints201803.0099.v1

MWCNTs were functionalized by adding 1 g of MWCNTs in APTES and toluene (1:9 v/v) solution. The mixture was refluxed at 105°C for 5 h and then was filtered and washed with acetone to remove any APTES remnant. The residue was then collected and dried in an oven at 105°C for 6 h. For loaded TiO_2 nanoparticles onto APTES-MWCNTs, the mixture was prepared by mixing 1 g of APTES-MWCNTs with 1 g of TiO_2 nanoparticles at a ratio of 1: 1 w/w. Then, the mixture was heated at 105°C for 6 h under reflux condition. After that, the residue was filtered, washed with deionized water and dried in an oven at 100°C for 24 h. The procedure was repeated for 1:2, 1:3, 1:4 and 1:5 ratio.

Characterization

X-ray diffractometer (XRD)

Samples were ground using mortar and pestle to become a fine powder. Then, the sample is put on glass slides as sample holder and lightly pressed with another glass slides to get a thin layer. X-ray diffractograms were recorded on a Rigaku D/max-2500 powder diffractometer with Cu-Kα source ($\lambda = 0.154$ nm, 40 kV, 40mA) and operating at a scanning rate of 2.00^0 min^{-1}. The diffraction spectra were obtained at the diffraction angle, 2Θ from 10^0 to 80^0 at room temperature, with a step interval of 10° step size.

Raman spectroscopy

Raman spectra were acquired using Jobin Yvon HR 800 (Excitation 514.532 nm, CCD) at a temperature range between 100 °C and 1800 °C at room temperature. The samples tested by Raman spectroscopy could be characterized when taken from the production system thus no need further preparation or treatment.

Preprints (www.preprints.org) | NOT PEER-REVIEWED | Posted: 14 March 2018 doi:10.20944/preprints201803.0099.v1

Transmission Electron Microscopy (TEM)

The images of samples were captured using TEM FEI Tecnai BioTWIN. Samples were suspended in ethanol by sonification and the resulting suspension was then drop dried onto carbon film coated TEM grids.

Energy Dispersive X-ray Spectroscopy

Energy dispersive x-ray spectroscopy was obtained by using EDX, Hitachi SU8000, Japan at the Hi-Tech Instrument Sdn. Bhd, Malaysia. For sample preparation, the samples were put on top of an aluminum sample stub and trapped with double-sided tape. The elemental were analyzed by production system.

Photocatalytic Degradation Activity

Photocatalytic activity was carried out in a photoreactor with 250 ml Pyrex beaker and open to air. The photoreactor was set up inside a closed home-made box and the interior of the box was lined up with aluminum foil for the reflective interior surface. The exterior surface of the box is opaque to outside light. The photocatalytic degradation experiment was obtained by adding the MWCNTs-APTES-TiO_2 into 100 ml of 20 ppm reactant solution. As for blank sample, an aliquot of 5 mL of reactant was withdrawn without the presence of any samples. Mixtures of photocatalyst powder with reactant solution were stored in a reactor and exposed under illumination of UV bench lamp (302 nm, 230V ~ 50Hz) for 3 hours. The aqueous solution was stirred during the experiment. At every 30 minutes of time intervals, 5 mL of the reactant solution was taken out using a syringe and filtered through 0.45 πm Millipore syringe filter. The solution was then transferred to a square cuvette and consequently place in the sample holder of UV-Vis spectrophotometer. The absorption

Preprints (www.preprints.org) | NOT PEER-REVIEWED | Posted: 14 March 2018 doi:10.20944/preprints201803.0099.v1

spectra were recorded via of UV-Vis spectrophotometer and the percentage of reactant degradation was calculated using the formula:

$$Degradation\ (\%) = \frac{(C_0 - C_t)}{C_0}\ x\ 100\ ,$$

where C_0 is the initial absorption of dye and C_t is the absorption of dye after the reaction at t time.

Results and Discussion

Characterization of MWCNTs-APTES-TiO₂

The XRD patterns of APTES-MWCNTs, TiO_2, and MWCNTs-APTES-TiO_2 at different ratios are shown in Figure 1. The APTES-MWCNTs exhibit two peaks present at 25° and 42°, corresponds to the (002) and (101) of CNT lattice, which confirmed the CNTs structure and hybridization of sp^2 atoms (Masipa et al. 2013). Another previous study also reported that the peak at 2θ = 25° corresponds to the (002) plane of graphite, and which indicate the interlayer stacking of graphene sheets at nano dimensions (Narendranath et al. 2014). Another study also clarified that peaks was classified as multi-walled carbon nanotubes (Krishnamurthy and Namitha 2013). The peaks present at 2θ = 38°, 48°, 54°, 55°, 63°, 69°, and 71 assigned to (101), (200), (105), (211), (204), (166), and (220), respectively are the characteristic of the crystallize anatase TiO_2 phase structure (Kim and Choi 2015, Safari and Gandomi-Ravandi 2014, Scheibe et al. 2009). The peaks for MWCNTs-APTES-TiO_2 (1:1) could not be clearly observe due to the main peak for MWCNTs overlaps with the main anatase TiO_2 peak at 2θ = 25° (de Morais et al. 2013, Golobostanfard and Abdizadeh 2014). Peaks of MWCNTs-APTES-TiO_2 at 2θ = 25°, 37°, 48°, and 54° assigned to the (101), (004), (200), and (211) planes, respectively, referring to anatase TiO_2 (Razali et al., 2017) (Mombeshora et al. 2015). A similar observation was also reported in a previous

Preprints (www.preprints.org) | NOT PEER-REVIEWED | Posted: 14 March 2018 doi:10.20944/preprints201803.0099.v1

study (Saleh et al. 2014). For MWCNTs-APTES-TiO_2 at different mass ratios (1:2, 1:3, 1:4 and 1:5) show the anatase TiO_2 nanoparticles were successfully loaded onto APTES-MWCNTs.

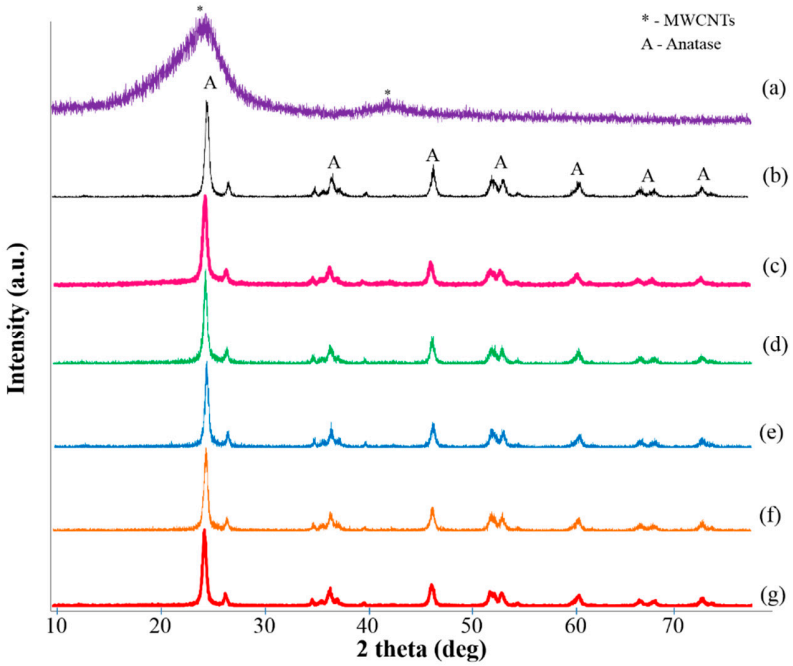

Figure 1: XRD patterns of (a) Functionalized-MWNTs, (b) TiO_2 nanoparticles (c) MWNTs-APTES-TiO_2 (1:1), (d) MWNTs-APTES-TiO_2 (1:2), (e) MWNTs-APTES-TiO_2 (1:3), (f) MWNTs-APTES-TiO_2 (1:4) and (g) MWNTs-APTES-TiO_2 (1:5).

The average crystallite size of anatase in the samples was calculated with the Scherrer formula using the anatase (101) diffraction peaks:

$$D = \frac{k\lambda}{\beta \cos \theta}$$

where D is the average crystallite size, k is a constant (0.89), λ is the wavelength of the X-ray radiation (0.154 nm), β is the band broadening (full width at half-maximum) and θ is the diffraction angle. Based on the previous study, the optimum crystallite sizes were ~20 – 25 nm for anatase and ~50 nm for brookite (Chen et al. 2015). Based on results of particle

Preprints (www.preprints.org) | NOT PEER-REVIEWED | Posted: 14 March 2018 doi:10.20944/preprints201803.0099.v1

sizes are shown in Table 1, it can be seen that there are no major differences in particle size with increasing amounts of TiO_2 with the average crystallite size in the range of 16 to 19 nm. Among the samples, MWCNTs-APTES-TiO_2 with ratio 1:2 has the highest crystallite size and is expected to be a good photocatalyst because it could provide a better contact point between the nanoparticles. Hence, this advantage provides a more efficient charge transport and faster photoinduction for the electron transfer (Yu et al. 2005b).

Table 1: Crystallite size of samples

Photocatalyst	Crystallite size (nm)
TiO_2	16.6
MWNTs-APTES-TiO_2 (1:1)	17.3
MWNTs-APTES-TiO_2 (1:2)	18.6
MWNTs-APTES-TiO_2 (1:3)	17.9
MWNTs-APTES-TiO_2 (1:4)	17.9
MWNTs-APTES-TiO_2 (1:5)	18.5

The Raman spectra of APTES-MWCNTs, TiO_2, and MWCNTs-APTES-TiO_2 at different ratios are shown in Figure 2. For APTES-MWCNTs show two peaks at ~1340 cm^{-1} and ~1580 cm^{-1} ascribed to D and G bands vibrations, respectively (Sheikh et al. 2015). The D band explained the distortions on the MWCNTs surface (Nuruzatulifah et at., 2012), while G band explains the crystalline nature of MWCNTs (Mansor et al. 2012). In addition, no peak of a radial breathing mode (RBM) observe in the range of 100 cm^{-1} to 350 cm^{-1} confirm that the synthesized CNTs is multi-walled (Masoumi et al. 2010). The peaks at 146 cm^{-1}, 197 cm^{-1}, 394 cm^{-1}, 401 cm^{-1}, 520 cm^{-1}, and 634 cm^{-1} shows the presence of TiO_2 anatase phase (Gonzalez 1996), which was supported by XRD data. The spectra of MWCNTs-APTES-TiO_2 for all ratios exhibit all the peaks of APTES-MWCNTs and pristine TiO_2, respectively, and thus can conclude that the APTES-MWCNTs loaded

Preprints (www.preprints.org) | NOT PEER-REVIEWED | Posted: 14 March 2018 doi:10.20944/preprints201803.0099.v1

197 TiO_2 were successfully synthesized. The intensity ratio (I_D/I_G) were measured to indicate a
198 number of structural defects on the sidewalls of the MWCNTs (Jeong et al. 2010, Osswald
199 et al. 2007). The I_D/I_G of MWCNTs-APTES-TiO_2 was found to be 1.09, 1.19, 1.15, 1.08
200 and 0.97 for 1:1, 1:2, 1:3, 1:4 and 1:5 ratios, respectively. Accordingly, the I_D/I_G decrease
201 because defects in MWCNTs have decreased due to titania binding to the oxygen groups
202 within the defect sites (Vigolo and Hérold 2011). Also, the previous study reported that the
203 low I_D/I_G ratio of multiwalled carbon nanotube-titania nanocomposites due to the low
204 amount of nanotubes and the large amount of titania that can bind and cover the defect sites
205 (Mombeshora et al. 2015)

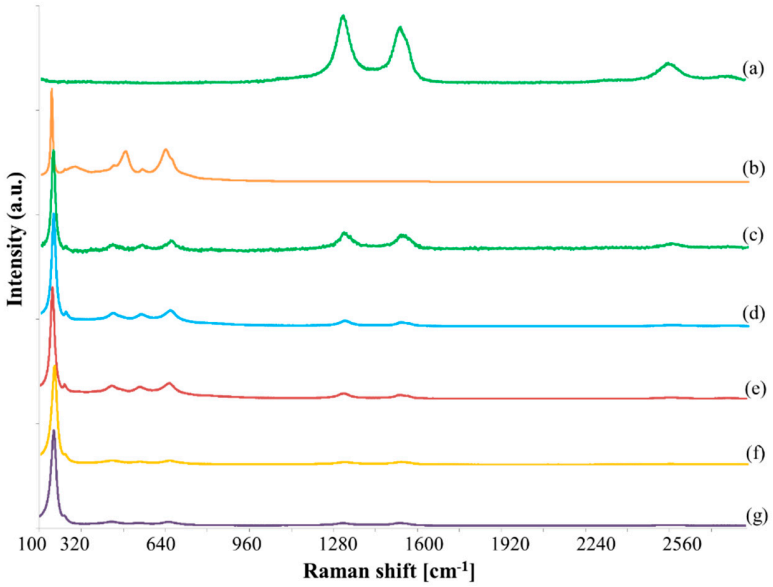

206
207 Figure 2: Raman Spectra (a) Functionalized-MWNTs, (b) TiO_2 nanoparticles (c) MWNTs-
208 APTES-TiO_2 (1:1), (d) MWNTs-APTES-TiO_2 (1:2), (e) MWNTs-APTES-TiO_2 (1:3), (f)
209 MWNTs-APTES-TiO_2 (1:4) and (g) MWNTs-APTES-TiO_2 (1:5).
210

211 TEM images of MWCNTs-APTES-TiO_2 in different mass ratios show that some of
212 the TiO_2 clusters were attached to functionalized-CNTs due to bonding between the
213 hydroxyl groups of TiO_2 and the amine groups of functionalized-MWCNTs (Figure 3).

Preprints (www.preprints.org) | NOT PEER-REVIEWED | Posted: 14 March 2018 doi:10.20944/preprints201803.0099.v1

Besides, it is well revealed that TiO_2 nanoparticles were attached on the surface of functionalized-MWCNTs (Fig. 3f). By inclusion of the higher amount of TiO_2 over functionalized-MWCNTs, it caused the surface of the MWCNTs to be much more covered with TiO_2 and limited the interaction between both samples.

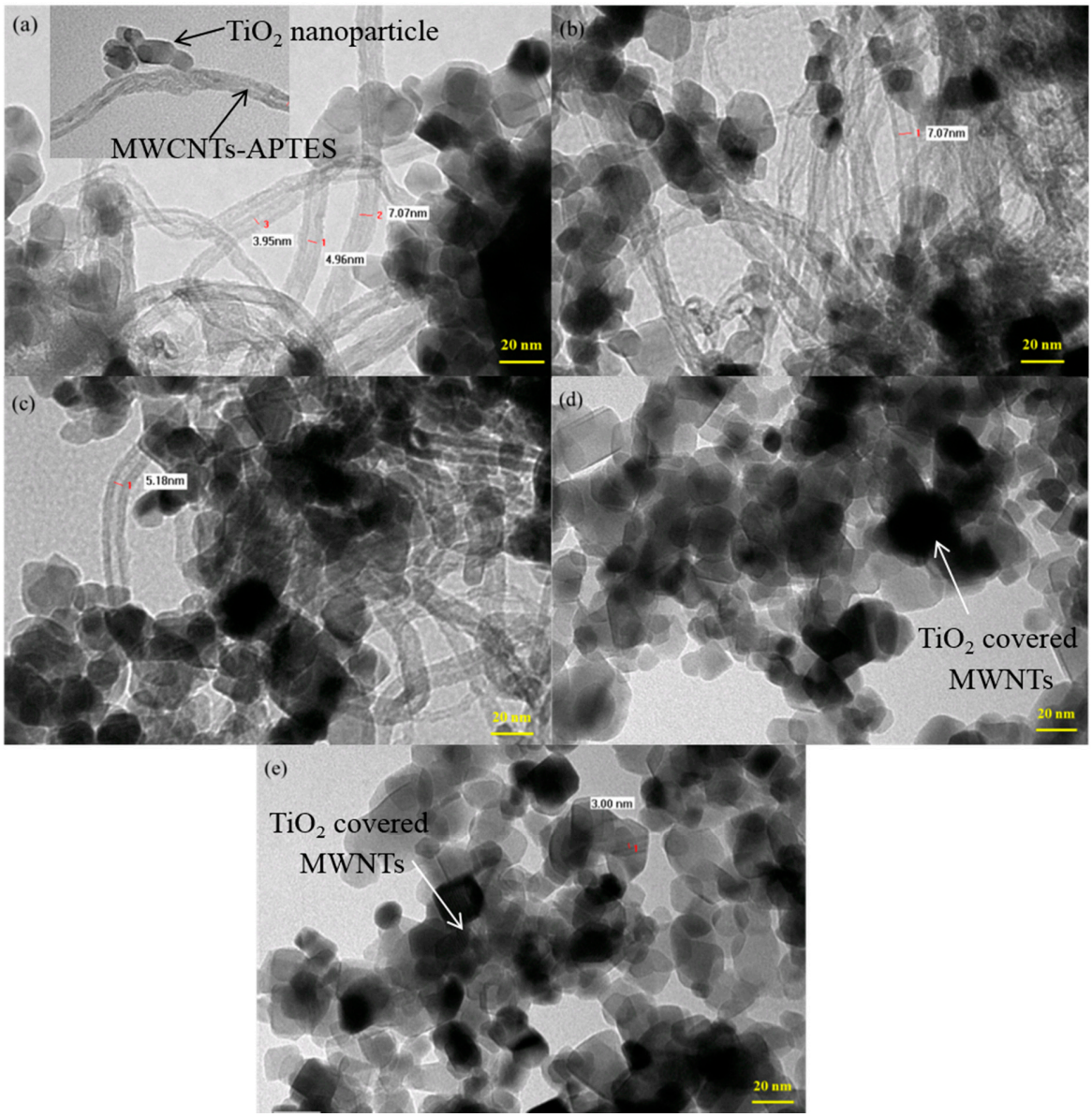

Figure 3 : TEM images of MWNTs-APTES-TiO_2 composites at different mass ratios (a) 1:1, (b) 1:2, (c) 1:3, (d) 1:4 and (e) 1:5

Preprints (www.preprints.org) | NOT PEER-REVIEWED | Posted: 14 March 2018 doi:10.20944/preprints201803.0099.v1

The elemental compositions of nanocomposites were analyzed with Energy-dispersive X-ray Spectroscopy (Table 2). The results obtained show that the amount of Ti increases as the TiO_2 content increased. It clearly shows that the amount of titanium was 24.38% and 43.03% for 1:1 and 1:5 ratio, respectively.

Table 2: Elemental analysis of samples

Photocatalyst	Element				
	C	O	Si	Ti	Au
TiO_2	-	-	-	-	-
MWNTs-APTES-TiO_2 (1:1)	37.26	20.24	1.72	24.38	16.40
MWNTs-APTES-TiO_2 (1:2)	35.30	21.51	1.88	26.24	15.07
MWNTs-APTES-TiO_2 (1:3)	24.59	26.39	0.94	35.62	12.45
MWNTs-APTES-TiO_2 (1:4)	13.41	27.53	0.16	36.90	22.00
MWNTs-APTES-TiO_2 (1:5)	-	32.36	0.60	43.03	24.01

Photocatalytic activity

Photodegradation of methyl orange (MO) exposed under UV light irradiation for 180 min is employed to estimate the photocatalytic activity of the prepared composites. The UV-Vis spectra of MO solution in the presence pure TiO_2 nanoparticles and MWCNTs-APTES-TiO_2 composites with 1:1, 1:2, 1:3, 1:4, 1:5 ratios are shown in Figure 4. It can be seen that a major absorbance can be observed at 464 nm in the initial UV-Vis spectra of MO, which is due to azo-linkage (Al-Qaradawi and Salman 2002). The degradation rate of each sample is shown in Figure 5. It can be seen that MWCNTs-APTES-TiO_2 shows major improvement in the degradation of MO compared to pure TiO_2. It also shows the highest efficiency at the mass ratio of MWCNTs:TiO_2 = 1:2. These results are reliable with previous studies that mentioned the suitable loading content of MWCNTs in applications is important to improve the photocatalytic activity of MWCNTs-TiO_2 (Yu et al. 2011). After 180 min, ~87% of the MO was degraded by MWCNTs-APTES-TiO_2 (1:2), followed by MWCNTs-APTES-TiO_2

Preprints (www.preprints.org) | NOT PEER-REVIEWED | Posted: 14 March 2018 doi:10.20944/preprints201803.0099.v1

(1:1) at 72%, MWCNTs-APTES-TiO_2 (1:3) at 70%, MWCNTs-APTES-TiO_2 (1:4) at 69%, MWCNTs-APTES-TiO_2 (1:5) at 67% and TiO_2 at 43%. The MWCNTs-APTES-TiO_2 is photocatalytically more active than TiO_2 because there are more hydroxyl radicals produced by MWCNTs-APTES-TiO_2 under UV. Thus, it could be suggested that MO was eliminated mainly by hydroxyl radical oxidation under UV light irradiation.

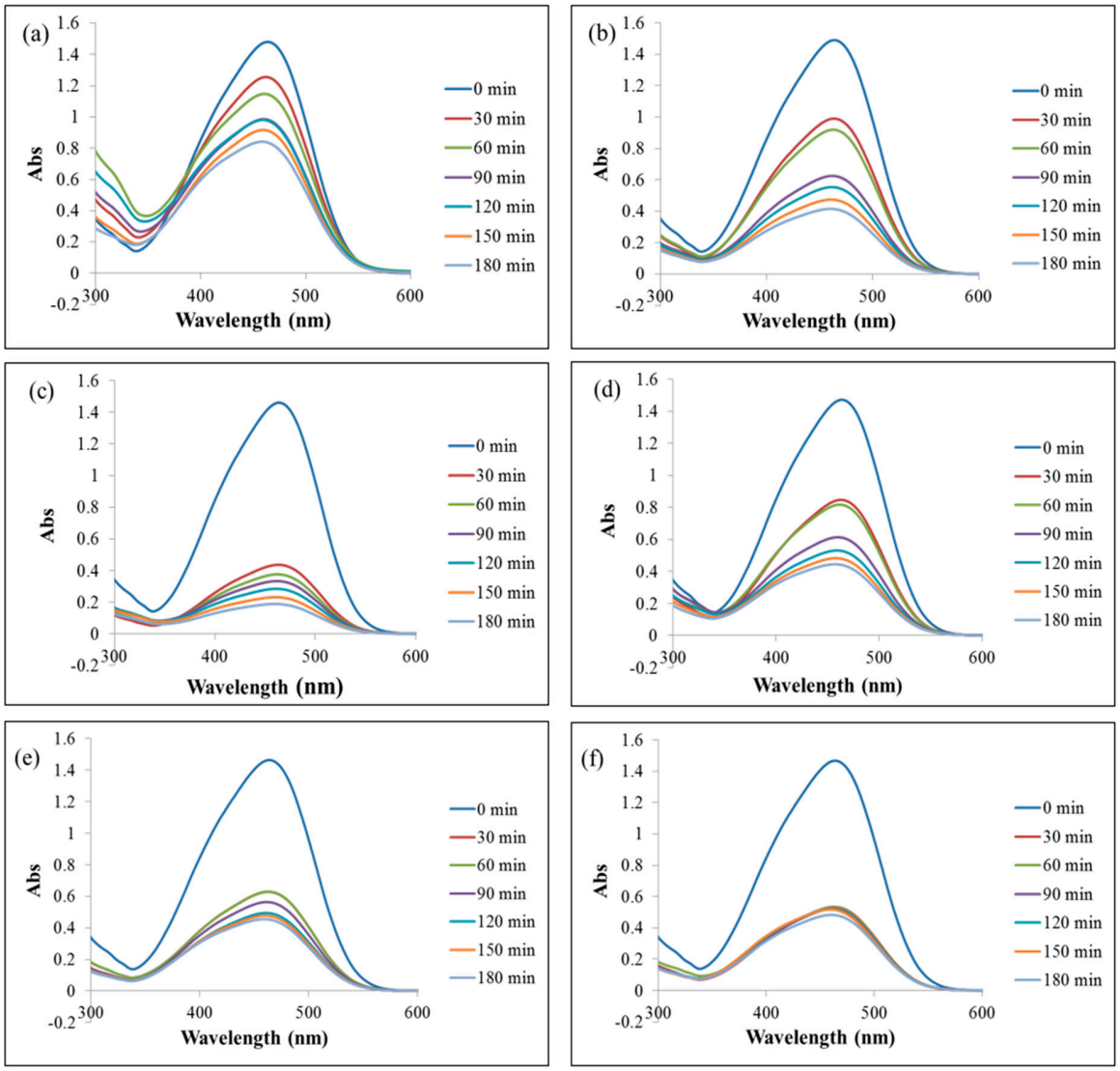

Figure 4: Uv-Vis spectra for the photocatalytic degradation of MO using (a) pure TiO_2 nanoparticles and MWNTs-APTES-TiO_2 composites in different mass ratios (b) 1:1, (c) 1:2, (d) 1:3, (e) 1:4 and (f) 1:5.

Preprints (www.preprints.org) | NOT PEER-REVIEWED | Posted: 14 March 2018 doi:10.20944/preprints201803.0099.v1

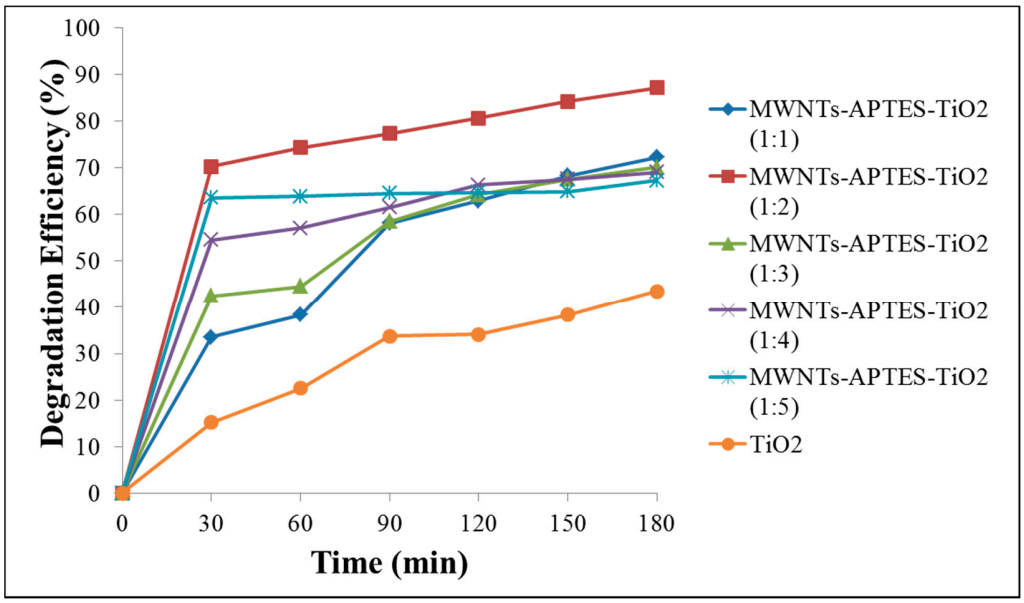

Figure 5: The degradation rate of MO in the presence of various composites under UV irradiation.

There are reasons proposed for the increased activity of MWCNTs-APTES-TiO_2 compared to pure TiO_2. Under UV light irradiations, electrons are excited from the valence band to the conduction band of TiO_2, thus creating a hole in the valence band (Czech et al. 2015). For pure TiO_2, most of these charges quickly recombine and only a small number of electrons and holes are trapped and participate in photocatalytic reactions resulting in low reactivity degradation of MO (Li and Gray 2007). For MWCNTs-APTES-TiO_2, TiO_2 nanoparticles are intimate contact with MWCNTs and the relative position of the MWCNTs conduction band edge permits the transfer of electrons from TiO_2 surface. Thus it allows the recombination, stabilization and charge separation. The excited electron can be shuttled freely along the conducting network of MWCNTs and transfer to the surface which react with water and oxygen to yield hydroxyl radical and oxidized MO. Higher the activity of the MWCNTs-APTES-TiO_2 photocatalyst depends on the longer holes on TiO_2 (Aazam 2014, Tseng et al. 2010).

Preprints (www.preprints.org) | NOT PEER-REVIEWED | Posted: 14 March 2018 doi:10.20944/preprints201803.0099.v1

Besides that, the presence of functionalized-MWCNTs provides a large number of reactive sites compared to pure TiO_2 (Cao et al. 2013). It allows larger adsorption of hydroxyl groups being a source of •OH radicals. Then, oxygen taking part in the process and adsorbed on the carbon nanotubes surface enable the formation of additional *OH radicals. Therefore, there are more hydroxyl radicals in the MWCNTs-APTES-TiO_2 than in TiO_2 (Czech et al. 2015, Yu et al. 2005a). Moreover, MO molecules can transfer from solution to the catalyst surface and be adsorbed by μ-μ conjugation between MO and MWCNTs-APTES-TiO_2. Also, because of that, the adsorptivity of MO on MWCNTs-APTES-TiO_2 increases and high efficiency in the photodegradation of MO compared to pure TiO_2 as a photocatalyst. Table 3 shows the results obtained in this study with those in the previously reported work on the various photocatalyst for degradation of MO in aqueous solution.

Table 3; Previously reported degradation rate of various photocatalyst on MO

Photocatalyst	Dye adsorbed	Time (min)	Degradation (%)	Reference
MWCNT/TiO_2	MB	100	76	(Zhao et al. 2013)
Activated carbon	MO	100	30	(Li et al. 2006)
TiO_2/AC	MO	100	77	(Li et al. 2006)
TiO_2-Ni	MO	120	77	(Zhang et al. 2010)
Pure TiO_2	MO	120	34	This study
MWCNTs-APTES-TiO_2	MO	120	81	This study

MB = Methylene blue, MO = Methyl orange

In the present study, zero, first- and second-order reaction kinetics were studied to know the degradation kinetics of MO by MWCNTs-APTES-TiO_2. The linear forms of kinetic model are represented by equation as follows,

Preprints (www.preprints.org) | NOT PEER-REVIEWED | Posted: 14 March 2018 doi:10.20944/preprints201803.0099.v1

- Zero-order reaction kinetics:

$$C_t = C_0 - k_0 t ,$$

- First-order reaction kinetics:

$$C_t = C_0 e^{-k_1 t}$$

- Second-order reaction kinetics:

$$1/C_t = 1/C_0 + k_2 t$$

where C_0 and C_t are the concentration of MO at initial and at the time, t, (mg L^{-1}), respectively; k_0, k_1 and k_2 is the rate constant of the zero, first and second order kinetic model, respectively. The values of k_0, k_1 and k_2 can be determined from the plots of C_t versus time, ln (C_0/C_t) against time and $1/C_t$ versus time, respectively.

The three kinetic models for the degradation of MO on functionalized-MWCNTs loaded titania are presented in Figure 6 and the kinetic parameters (k_0, k_1 and k_2) and correlation coefficients (R^2) were calculated and were summarized in Table 4. By comparing the regression coefficient obtained, it can be seen that R^2 of second-order reaction kinetic was obviously higher than zero and first-order kinetic model. Therefore, it was feasible for the applicability of the second-order kinetic model to describe the degradation process of MO on MWCNTs-APTES-TiO_2. Then, the results obtained were analyzed by the half-lives equation as follows (Kavitha and Namasivayam 2007):

- Zero-order reaction kinetics:

$$t_{1/2} = C_0 / 2k_0 ,$$

- First-order reaction kinetics:

Preprints (www.preprints.org) | NOT PEER-REVIEWED | Posted: 14 March 2018 doi:10.20944/preprints201803.0099.v1

$$t_{1/2} = 0.6934/k_1$$

- Second-order reaction kinetics:

$$t_{1/2} = 1/k_2 C_0$$

where k_0, k_1 and k_2 is the rate constant of the zero, first and second order kinetic model, respectively.

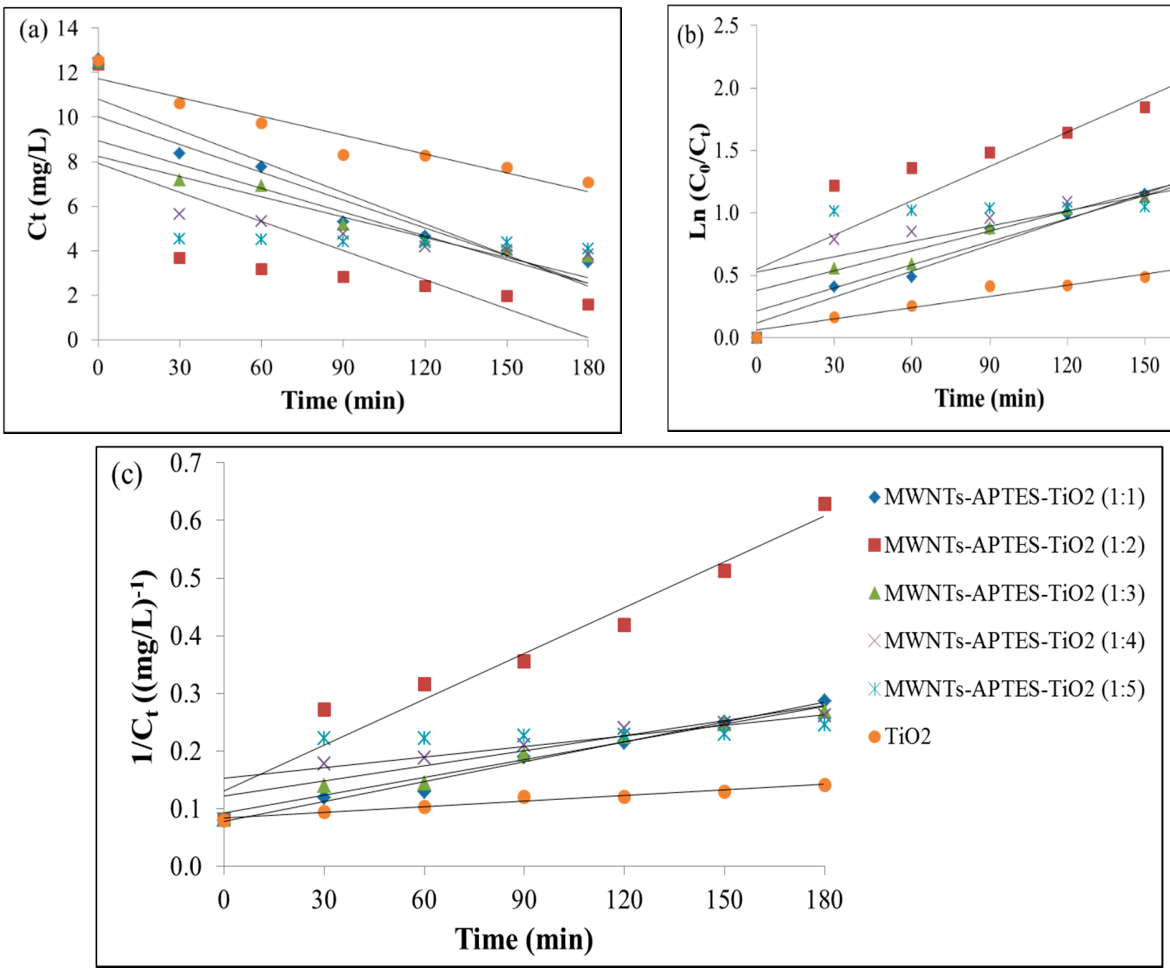

Preprints (www.preprints.org) | NOT PEER-REVIEWED | Posted: 14 March 2018 doi:10.20944/preprints201803.0099.v1

Table 4: Degradation rates and kinetic parameters of MO degradation

Degradation (%)	Zero Order		First Order		Second order	
	k_0	R^2	k_1	R^2	k_2	R^2
43.6	0.0282	0.9162	0.00498	0.9494	0.0834	0.9701
72.3	0.0467	0.8782	0.01075	0.9617	0.0012	0.9867
87.1	0.0435	0.5636	0.02722	0.7909	0.0026	0.9525
70.1	0.0415	0.7845	0.01324	0.9055	0.0010	0.9734
69.0	0.0357	0.5920	0.01792	0.7208	0.0009	0.8512
67.2	0.0303	0.4167	0.02164	0.4495	0.0006	0.4960

The $t_{1/2}$ experiment was determined from the graph of C_t versus time for ratio 1:2 (Figure 7). For $t_{1/2}$ calculation, the value for zero, first and second-order are 142, 76 and 29 min, respectively. Meanwhile, the value for $t_{1/2}$ experiment from the graph is 22 min. It clearly shows the $t_{1/2}$ experiment close with $t_{1/2}$ for second order and proved that the degradation of MO on MWCNTs-APTES-TiO_2 followed the second order kinetic model.

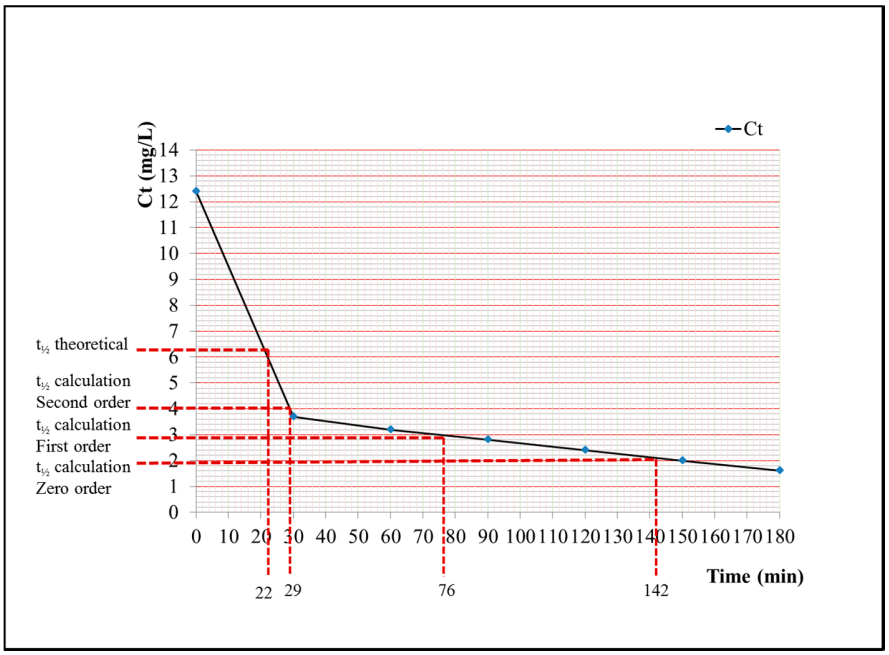

Figure 7: Graph of C_t versus time for MWNTs-APTES-TiO_2 at 1:2 ratio

 doi:10.20944/preprints201803.0099.v1

Conclusions

A new kind of nanocomposite photocatalyst by using functionalized-MWCNTs as a support for TiO_2 nanoparticles on getting high degradation rates of MO were successfully synthesized using the hydrothermal method. It is found that the degradation of MO solution using MWCNTs-APTES-TiO_2 was recorded at 87% after 180 min, which was higher than pure TiO_2 (43%). The presence of functionalized-MWCNTs accelerated the degradation of MO due to an inhibitory effect of electron/holes recombination, which increase the formation of •OH radicals. The MWCNTs-APTES-TiO_2 nanocomposites with mass ratio 1:2 (MWCNTs:TiO_2) exhibit the highest photocatalytic activity during the degradation of MO dye compared to other ratios and the degradation kinetics follow the second-order kinetic model with a high correlation coefficient (> 0.95). The results of this research highlighted MWCNTs-APTES-TiO_2 nanocomposite as an effective photocatalyst and towards facilitating its application in environmental problems.

Acknowledgements

The authors are grateful to the School of Fundamental Science, Centre Laboratory, and University Malaysia Terengganu for providing the facilities for this experiment.

Compliance with Ethical Standards

Funding: This study was funded by Ministry of Higher Education of Malaysia under the Fundamental Research Grant Scheme (FRGS) vote 55924 and 59358.

371

372 **Conflict of Interest**: The authors declare that they have no conflict of interest.

373 **References**

374 Aazam, E. (2014) Visible light photocatalytic degradation of thiophene using Ag–TiO 2/multi-walled carbon
375 nanotubes nanocomposite. Ceramics International 40: 6705-6711.
376 Ahmad, A., Razali, M.H., Mamat, M., Mehamod, F.S.B. and Amin, K.A.M. (2017) Adsorption of methyl
377 orange by synthesized and functionalized-CNTs with 3-aminopropyltriethoxysilane loaded TiO 2
378 nanocomposites. Chemosphere 168: 474-482.
379 Al-Qaradawi, S. and Salman, S.R. (2002) Photocatalytic degradation of methyl orange as a model
380 compound. Journal of Photochemistry and photobiology A: Chemistry 148: 161-168.
381 Cao, Q., Yu, Q., Connell, D.W. and Yu, G. (2013) Titania/carbon nanotube composite (TiO2/CNT) and its
382 application for removal of organic pollutants. Clean Technologies and Environmental Policy 15: 871-
383 880.
384 Chen, W.-T., Chan, A., Jovic, V., Sun-Waterhouse, D., Murai, K.-i., Idriss, H. and Waterhouse, G.I. (2015)
385 Effect of the TiO2 Crystallite Size, TiO2 Polymorph and Test Conditions on the Photo-Oxidation Rate
386 of Aqueous Methylene Blue. Topics in Catalysis 58: 85-102.
387 Chen, Y.-F., Lee, C.-Y., Yeng, M.-Y. and Chiu, H.-T. (2003) The effect of calcination temperature on the
388 crystallinity of TiO 2 nanopowders. Journal of Crystal Growth 247: 363-370.
389 Czech, B., Buda, W., Pasieczna-Patkowska, S. and Oleszczuk, P. (2015) MWCNT–TiO 2–SiO 2
390 nanocomposites possessing the photocatalytic activity in UVA and UVC. Applied Catalysis B:
391 Environmental 162: 564-572.
392 de Morais, A., Loiola, L.M., Benedetti, J.E., Goncalves, A.S., Avellaneda, C.A., Clerici, J.H., Cotta, M.A. and
393 Nogueira, A.F. (2013) Enhancing in the performance of dye-sensitized solar cells by the
394 incorporation of functionalized multi-walled carbon nanotubes into TiO 2 films: The role of MWCNT
395 addition. Journal of Photochemistry and Photobiology A: Chemistry 251: 78-84.
396 Djokić, V.R., Marinković, A.D., Ersen, O., Uskoković, P.S., Petrović, R.D., Radmilović, V.R. and Janaćković,
397 D.T. (2014) The dependence of the photocatalytic activity of TiO 2/carbon nanotubes
398 nanocomposites on the modification of the carbon nanotubes. Ceramics International 40: 4009-
399 4018.
400 Fujishima, A., Rao, T.N. and Tryk, D.A. (2000) Titanium dioxide photocatalysis. Journal of Photochemistry
401 and Photobiology C: Photochemistry Reviews 1: 1-21.
402 Gao, B., Chen, G.Z. and Puma, G.L. (2009) Carbon nanotubes/titanium dioxide (CNTs/TiO 2)
403 nanocomposites prepared by conventional and novel surfactant wrapping sol–gel methods
404 exhibiting enhanced photocatalytic activity. Applied Catalysis B: Environmental 89: 503-509.
405 Golobostanfard, M.R. and Abdizadeh, H. (2014) Hierarchical sol–gel derived porous titania/carbon
406 nanotube films prepared by controlled phase separation. Microporous and Mesoporous Materials
407 183: 74-80.
408 Gonzalez, R.J. (1996) Raman, infrared, X-ray, and EELS studies of nanophase titania, Virginia Polytechnic
409 Institute and State University.
410 Haque, E., Jun, J.W. and Jhung, S.H. (2011) Adsorptive removal of methyl orange and methylene blue from
411 aqueous solution with a metal-organic framework material, iron terephthalate (MOF-235). Journal
412 of hazardous materials 185: 507-511.

413 Harris, P.J.F. (2009) Carbon nanotube science: synthesis, properties and applications, Cambridge
414 University Press.
415 Hoffmann, M.R., Martin, S.T., Choi, W. and Bahnemann, D.W. (1995) Environmental applications of
416 semiconductor photocatalysis. Chemical reviews 95: 69-96.
417 Hone, J., Llaguno, M., Biercuk, M., Johnson, A., Batlogg, B., Benes, Z. and Fischer, J. (2002) Thermal
418 properties of carbon nanotubes and nanotube-based materials. Applied physics A 74: 339-343.
419 Jeong, Y., Kim, J. and Lee, G.-W. (2010) Optimizing functionalization of multiwalled carbon nanotubes
420 using sodium lignosulfonate. Colloid and Polymer Science 288: 1-6.
421 Jiang, G., Zheng, X., Wang, Y., Li, T. and Sun, X. (2011) Photo-degradation of methylene blue by multi-
422 walled carbon nanotubes/TiO 2 composites. Powder Technology 207: 465-469.
423 Kavitha, D. and Namasivayam, C. (2007) Experimental and kinetic studies on methylene blue adsorption
424 by coir pith carbon. Bioresource Technology 98: 14-21.
425 Kim, S.P. and Choi, H.C. (2015) Preparation of Carbon-Nanotube-supported TiO2 for Enhanced Dye-
426 degrading Photocatalytic Activity. Bulletin of the Korean Chemical Society 36: 258-264.
427 Krishnamurthy, G. and Namitha, R. (2013) A Novel Method of Synthesis of Carbon Nanotube by
428 Hydrothermal Process. International Journal of Science Research 1: 358-362.
429 Kubacka, A., Fernandez-Garcia, M. and Colon, G. (2011) Advanced nanoarchitectures for solar
430 photocatalytic applications. Chemical reviews 112: 1555-1614.
431 Legrini, O., Oliveros, E. and Braun, A. (1993) Photochemical processes for water treatment. Chemical
432 reviews 93: 671-698.
433 Li, G. and Gray, K.A. (2007) The solid–solid interface: explaining the high and unique photocatalytic
434 reactivity of TiO 2-based nanocomposite materials. Chemical physics 339: 173-187.
435 Li, Y., Li, X., Li, J. and Yin, J. (2006) Photocatalytic degradation of methyl orange by TiO 2-coated activated
436 carbon and kinetic study. Water research 40: 1119-1126.
437 Ling Tan, T., Bee Abd Hamid, S. and Wei Lai, C. (2015) Modification of Multi-walled Carbon Nanotubes
438 with Nanoparticles for High Photocatalytic Activity. Current Nanoscience 11: 504-508.
439 Mansor, N.B.A., Tessonnier, J.-P., Rinaldi, A., Reiche, S. and Kutty, M. (2012) Chemically modified multi-
440 walled carbon nanotubes (MWCNTs) with anchored acidic groups. Sains Malaysiana 41: 603-609.
441 Masipa, P.M., Magadzu, T. and Mkhondo, B. (2013) Decoration of multi-walled carbon nanotubes by metal
442 nanoparticles and metal oxides using chemical evaporation method. South African Journal of
443 Chemistry 66: 00-00.
444 Masoumi, M., Mehrnia, M.R., Montazer-Rahmati, M. and Rashidi, A.M. (2010) Templated growth of
445 carbon nanotubes on nickel loaded mesoporous MCM-41 and MCM-48 molecular sieves.
446 International Journal of Nanoscience and Nanotechnology 6: 88-96.
447 Mombeshora, E.T., Simoyi, R., Nyamori, V.O. and Ndungu, P.G. (2015) Multiwalled carbon nanotube-
448 titania nanocomposites: Understanding nano-structural parameters and functionality in dye-
449 sensitized solar cells. South African Journal of Chemistry 68: 153-164.
450 Nainani, R., Thakur, P. and Chaskar, M. (2012) Synthesis of silver doped TiO2 nanoparticles for the
451 improved photocatalytic degradation of methyl orange. Journal of Materials Science and
452 Engineering B 2: 52-58.
453 Narendranath, S., Ramesh, M.R., Chakradhar, D., Doddamani, M., Bontha, S., Krishnamurthy, G., Namitha,
454 R. and Agarwal, S. (2014) International Conference on Advances in Manufacturing and Materials
455 Engineering, ICAMME 2014Synthesis of Carbon Nanotubes and Carbon Spheres and Study of their
456 Hydrogen Storage Property by Electrochemical Method. Procedia Materials Science 5: 1056-1065.
457 Nuruzatulifah Bt Asari Mansor, J.-P.T., Ali Rinaldi, Sylvia Reiche (2012) Chemically modified multi-walled
458 carbon nanotubes (MWCNTs) with anchored acidic groups. Sains Malaysiana 41.
459 Osswald, S., Havel, M. and Gogotsi, Y. (2007) Monitoring oxidation of multiwalled carbon nanotubes by
460 Raman spectroscopy. Journal of Raman Spectroscopy 38: 728-736.

Pelaez, M., Nolan, N.T., Pillai, S.C., Seery, M.K., Falaras, P., Kontos, A.G., Dunlop, P.S., Hamilton, J.W., Byrne, J.A. and O'shea, K. (2012). A review on the visible light active titanium dioxide photocatalysts for environmental applications. Applied Catalysis B: Environmental 125: 331-349.

Razali, M. H., Noor, A.F.M., Yusoff, M. (2017). Hydrothermal synthesis and characterization of Cu^{2+}/F- co-doped titanium dioxide (TiO_2) nanotubes as photocatalyst for methyl orange degradation. Science of Advanced Materials. 9(6), pp. 1032-1041

Safari, J. and Gandomi-Ravandi, S. (2014) Carbon nanotubes supported by titanium dioxide nanoparticles as recyclable and green catalyst for mild synthesis of dihydropyrimidinones/thiones. Journal of Molecular Structure 1065: 241-247.

Saleh, T.A., Siddiqui, M.N. and Al-Arfaj, A.A. (2014) Synthesis of multiwalled carbon nanotubes-titania nanomaterial for desulfurization of model fuel. Journal of Nanomaterials 2014: 194.

Scheibe, B., Borowiak-Palen, E. and Kalenczuk, R. (2009) Effect of the silanization processes on the properties of oxidized multiwalled carbon nanotubes. Acta Physica Polonica A 116: S150-S155.

Sheikh, F.A., Macossay, J., Cantu, T., Zhang, X., Shamshi Hassan, M., Esther Salinas, M., Farhangi, C.S., Ahmad, H., Kim, H. and Bowlin, G.L. (2015) Imaging, spectroscopy, mechanical, alignment and biocompatibility studies of electrospun medical grade polyurethane (Carbothane™ 3575A) nanofibers and composite nanofibers containing multiwalled carbon nanotubes. Journal of the Mechanical Behavior of Biomedical Materials 41: 189-198.

Shitole, K.D., Nainani, R.K. and Thakur, P. (2013) Preparation, characterisation and photocatalytic applications of TiO2-MWCNTs composite. Defence Science Journal 63: 435-441.

Tseng, Y.-H., Yen, C.-Y., Yen, M.-Y. and Ma, C.-C. (2010) Effects of the acid pretreated multi-walled carbon nanotubes on the photocatalytic capacity of TiO 2/multi-walled carbon nanotubes nanocomposites. IET Micro & Nano Letters 5: 1-6.

Vigolo, B. and Hérold, C. (2011) Processing Carbon Nanotubes, INTECH Open Access Publisher.

Wu, C.-H., Kuo, C.-Y. and Chen, S.-T. (2013) Synergistic effects between TiO2 and carbon nanotubes (CNTs) in a TiO2/CNTs system under visible light irradiation. Environmental technology 34: 2513-2519.

Xu, Y.-J., Zhuang, Y. and Fu, X. (2010) New insight for enhanced photocatalytic activity of TiO2 by doping carbon nanotubes: a case study on degradation of benzene and methyl orange. The Journal of Physical Chemistry C 114: 2669-2676.

Yu, J., Ma, T. and Liu, S. (2011) Enhanced photocatalytic activity of mesoporous TiO 2 aggregates by embedding carbon nanotubes as electron-transfer channel. Physical Chemistry Chemical Physics 13: 3491-3501.

Yu, Y., Jimmy, C.Y., Chan, C.-Y., Che, Y.-K., Zhao, J.-C., Ding, L., Ge, W.-K. and Wong, P.-K. (2005a) Enhancement of adsorption and photocatalytic activity of TiO 2 by using carbon nanotubes for the treatment of azo dye. Applied Catalysis B: Environmental 61: 1-11.

Yu, Y., Ma, L.-L., Huang, W.-Y., Du, F.-P., Jimmy, C.Y., Yu, J.-G., Wang, J.-B. and Wong, P.-K. (2005b) Sonication assisted deposition of Cu 2 O nanoparticles on multiwall carbon nanotubes with polyol process. Carbon 43: 670-673.

Zhang, Y., Wan, J. and Ke, Y. (2010) A novel approach of preparing TiO 2 films at low temperature and its application in photocatalytic degradation of methyl orange. Journal of hazardous materials 177: 750-754.

Zhao, D., Yang, X., Chen, C. and Wang, X. (2013) Enhanced photocatalytic degradation of methylene blue on multiwalled carbon nanotubes–TiO 2. Journal of Colloid and interface Science 398: 234-239.